

**Dieses Dokument ist eine Zweitveröffentlichung (Verlagsversion) /  
This is a self-archiving document (published version):**

Tony Henseleit, Markas Sudzius, Hartmut Fröb, Karl Leo

**Coherent perfect absorption in oneport devices with wedged organic thin-film absorbers**

**Erstveröffentlichung in / First published in:**

*SPIE Organic Photonics + Electronics*. San Diego, 2018. Bellingham: SPIE, Vol. 10736 [Zugriff am: 23.05.2019].

DOI: <https://doi.org/10.1117/12.2321082>

Diese Version ist verfügbar / This version is available on:

<https://nbn-resolving.org/urn:nbn:de:bsz:14-qucosa2-351769>

„Dieser Beitrag ist mit Zustimmung des Rechteinhabers aufgrund einer (DFGgeförderten) Allianz- bzw. Nationallizenz frei zugänglich.“

This publication is openly accessible with the permission of the copyright owner. The permission is granted within a nationwide license, supported by the German Research Foundation (abbr. in German DFG).

[www.nationallizenzen.de/](http://www.nationallizenzen.de/)

# PROCEEDINGS OF SPIE

[SPIDigitalLibrary.org/conference-proceedings-of-spie](https://SPIDigitalLibrary.org/conference-proceedings-of-spie)

## Coherent perfect absorption in one-port devices with wedged organic thin-film absorbers

Tony Henseleit, Markas Sudzius, Hartmut Fröb, Karl Leo

Tony Henseleit, Markas Sudzius, Hartmut Fröb, Karl Leo, "Coherent perfect absorption in one-port devices with wedged organic thin-film absorbers," Proc. SPIE 10736, Organic Light Emitting Materials and Devices XXII, 107361T (14 September 2018); doi: 10.1117/12.2321082

**SPIE.**

Event: SPIE Organic Photonics + Electronics, 2018, San Diego, California, United States

# Coherent perfect absorption in one-port devices with wedged organic thin film absorbers

Tony Henseleit, Markas Sudzius, Hartmut Fröb, and Karl Leo

Dresden Integrated Center for Applied Physics and Photonic Materials (IAPP) and Institute for Applied Physics, Technische Universität Dresden, 01062 Dresden, Germany

## ABSTRACT

We are using organic small molecules as absorbing material to investigate coherent perfect absorption in layered thin-film structures. Therefore we realize strongly asymmetric resonator structures with a high optical quality dielectric distributed Bragg reflector and thermally evaporated wedged organic materials on top. We investigate the optical properties of these structures systematically by selective optical pumping and probing of the structure. By shifting the samples along the wedge, we demonstrate how relations of phase and amplitude of all waves can be tuned to achieve coherent perfect absorption. Thus almost all incident radiation dissipates in the thin organic absorbing layer. Furthermore, we show how these wedged structures on a high-quality reflective dielectric mirror can be used to determine optical dispersion relations of absorbing materials in a broad spectral range. This novel approach does not require any specific a priori knowledge on the absorbing film.

**Keywords:** Coherent perfect absorption, organic thin films, optical resonators, optical dispersion relations

## 1. INTRODUCTION

For many optical and photonic devices, such as solar cells, photodetectors and photosensors, and optically pumped lasers, enhancement of absorption is very important.<sup>1</sup> Usually this can be achieved in thin layered planar structures with thickness in the wavelength range by carefully choosing the device structure.<sup>2</sup> In these structures, materials as well as layer thicknesses need to be chosen to achieve destructive interference for the total reflection from the structure in order to have all incident radiation getting absorbed within a pre-determined specific absorbing layer. Several theoretical and experimental reports on planar and corrugated systems using metals, Tamm states, J-aggregates, laser dyes or absorptive polymers showing enhanced absorption of the light were done in the past.<sup>2-8</sup>

Coherent perfect absorption (CPA) in two-port devices is referred to as time-reversed lasing at threshold and closely related to coherent absorption in one-port devices, which is often understood as critical coupling of light.<sup>2,9-14</sup> There will be no further differentiation between both approaches in this work because each of them require a precise control of phase and intensity relations to match the optical properties of the absorbing materials. Once the efficiency of absorption of light reaches values close to 100%, we will refer to it as CPA. Either way numerical investigation of coherent absorption in the system can be done by evaluating the optical response with standard characteristic matrices.<sup>15,16</sup>

## 2. ONE-PORT DEVICE STRUCTURE

### 2.1 Structure design and sample preparation

In this work, we are focusing on the one-port device, which is characterized by the fact that there just one input beam. To realize a one-port coherent perfect absorber as simple as possible, we use a structure consisting of an asymmetric cavity with a perfectly reflecting mirror on one side. The opposite side of the structure is coupled to the single input channel. For an optimal tuned absorption of the cavity, the reflection from the mirror and the reflection from the front face of the structure are destructively interfering, leading to the incident radiation being perfectly absorbed in the structure. To achieve this it is necessary to minimize the losses caused by transmission and therefore to use highly reflective structure.

We fabricated our devices on distributed Bragg reflectors (DBRs), which consist of 21 dielectric layers out of SiO<sub>2</sub> and TiO<sub>2</sub> alternately thermally evaporated with an electron beam. The first and last layer is always made

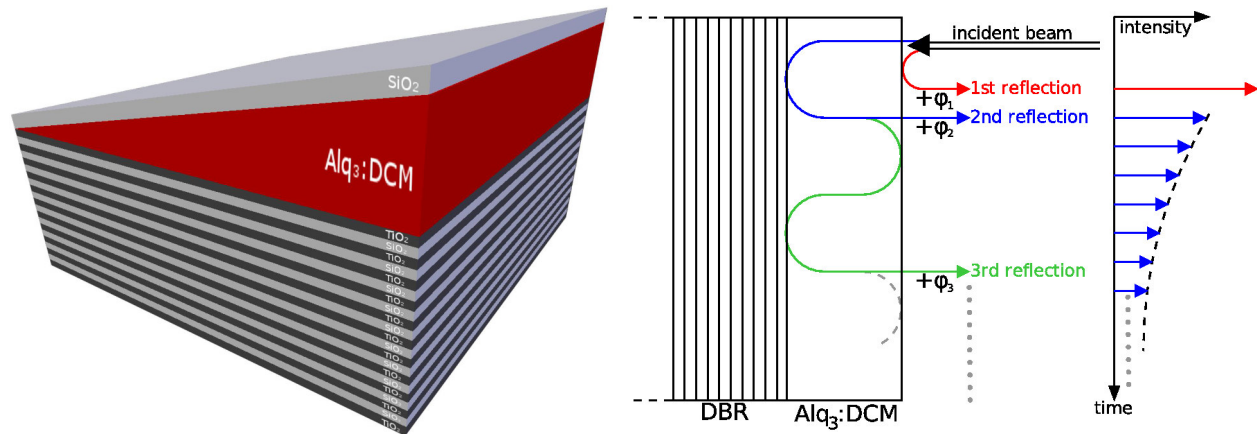


Figure 1. Left: Schematics of samples with one-port device structure consisting of a DBR with wedged organics and a capping layer on top. Right: Schematics of the working principle of coherent absorption in a one-port device structure.

from  $\text{TiO}_2$ . The organic absorbing material on top of the DBR is a mixture of Tris(8-hydroxyquinoline)aluminum ( $\text{Alq}_3$ ) and 4-(dicyanomethylene)-2-methyl-6-(p-dimethylaminostyryl)-4H-pyran (DCM), which is widely known as an excellent gain medium for optically pumped solid state organic microcavity lasers.<sup>17,18</sup> Both materials are thermally co-evaporated at the same time with roughly two weight percent of DCM in the mixture. This fraction can be achieved by adjusting the deposition rates through the crucible temperatures of the materials. The design wavelength of the DBRs in our structure is matched to the maximum of absorption in the absorbing materials which leaves us with two different types of samples. Structure “A” is matched to the absorption maximum of  $\text{Alq}_3$  and structure “B” is matched to DCM. The absorbing layer itself is a wedged layer giving a smooth phase control in our measurements by shifting the sample along the wedge but with a sufficiently small angle to still ensure the whole structure works as a planar device.<sup>19</sup> On top of the wedged organics a silicon dioxide capping layer is added to minimize degradation from reactions with the environment. The thickness of this capping layer equals half of the design wavelength of the respective structure. A schematic of the whole sample structure is shown in figure 1 on the left.

## 2.2 Working principle

On the right side, figure 1 schematically shows the working principle of a one-port device with all beams in real space and time domain taking intensities and phase relations into account. An incident beam (black) illuminates the structure from one side and is split up in a first reflected (red arrow) and a transmitted beam (blue arrow). The transmitted beam part passes the absorbing layer and is then reflected by the DBR where the transmission is neglected due to the high reflectivity the DBR inside the stopband.<sup>20</sup> Back at the structure surface the beam is again split into a transmitted (blue arrow) and reflected (green arrow) part. This continues for an infinite number of round trips with the intensity decreasing during each circulation. The phase difference  $\phi_i$  of each reflection from the surface is well defined by absorbing layer thickness and by the dispersion relations of the organic absorber. Now the coherent superposition of all reflections that have passed the absorbing layer (blue and green arrows) interferes with the initial reflection (red arrow). For destructive interference it results in the overall reflection to vanish. The energy therefore has to dissipate in the structure leading to 100% absorption in the device. This is called coherent perfect absorption.

The phasor diagram in figure 2 shows the different reflected waves with differently colored arrows with their length corresponding to their intensity. The direction shows the phase shift of the consecutively reflected waves compared to the incident beam. Therefore the initial reflection (red arrow) gets a shift of  $\phi_1 = \pi$  because the refractive index of the one-port device is larger than the index of the environment. The contiguous arrows form a path and in case of CPA this path closes asymptotically with its shape being defined by physical and optical properties of the absorbing layer. This occurs only if the thickness of the absorbing layer and its material are chosen appropriately.

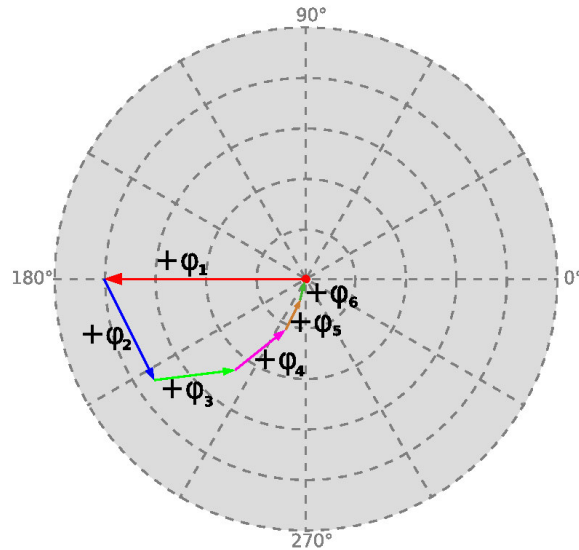


Figure 2. Phasor diagram schematically showing phase and amplitude of subsequent reflections in a one-port device as in figure 1 for coherent absorption.

### 3. COHERENT PERFECT ABSORPTION FOR WHITE LIGHT EXCITATION

#### 3.1 CPA in matrix material and CPA in dopant

Structure “A” shows under perpendicular excitation with white light a reflectance as in figure 3. The experimental data on the left hand side is shown in comparison to data from simulations with the transfer matrix method on the right. The stopband of the structure is marked on top of both plots. Because of the negligible transmission through the DBR in the stopband region there are no losses in terms of intensity. Apart from some small deviations in the sideband, the experimental reflectance is in very good agreement with the theoretical one. The artifacts for short wavelengths in the experimental data originate from spectral limitations of the used white light source.

For an increasing wedge thickness of the absorbing organic layer, there are really pronounced oscillations in reflectance which shows the interferometric nature of coherent absorption in this structure. Especially in the stopband, where the transmission almost vanishes as mentioned before, a reflection close to zero indicates almost perfect absorption. This can be seen both experimentally and theoretically for specific thicknesses. For an optical thickness of round about 1.15 times the design wavelength and an excitation wavelength around 400 nm the really low reflectance indicates, that CPA can be achieved in a one-port device structure with Alq<sub>3</sub> as an organic absorbing layer.

As for structure “A” the same investigations were done for structure “B” in order to see if coherent absorption is present in DCM as well. The results are shown in figure 4 again with the experimental data on the left and transfer-matrix calculations on the right. Both correspond again very well, especially in the stopband. Also interference is very pronounced, but the presence of coherent absorption is less obvious as for structure “A”. From the very good agreements between experimental and theoretical data in both structures it turns out that the mathematical models, that we used for our simulations, can describe the underlying physics properly including coherent absorption as an extreme case.<sup>21</sup>

#### 3.2 Polarization dependency

Structure “A” was also investigated under oblique excitation with white light, to see if coherent absorption is still possible under these conditions and how it is affected by the polarization of the incident light. For non-perpendicular illumination of the sample the reflected waves are spatially separated and the superposition of reflected waves and therefore coherent absorption might not come about. The absorbance of p-polarized and

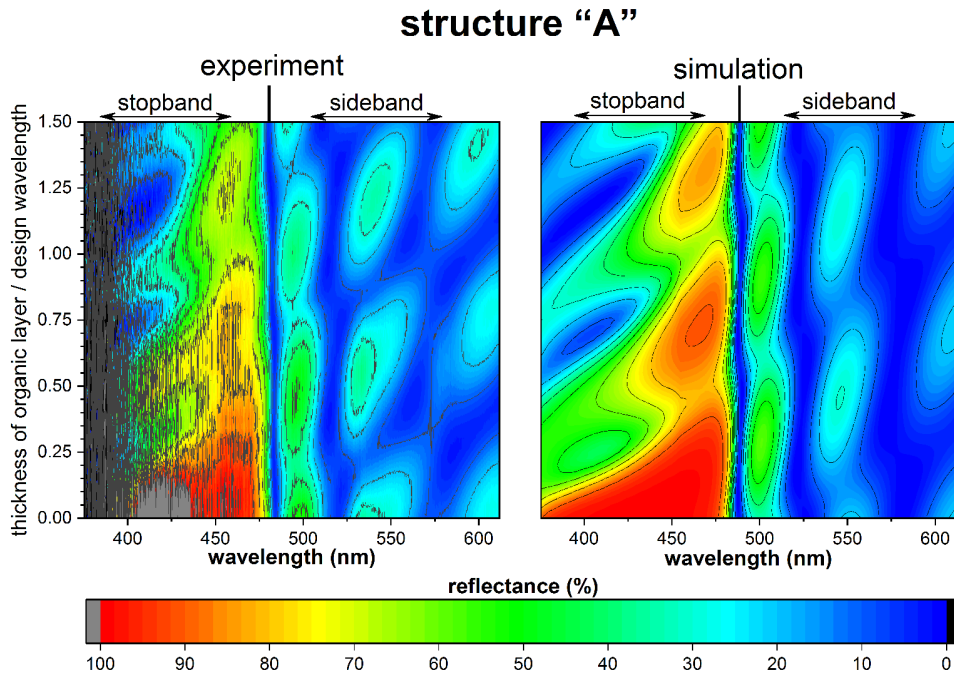


Figure 3. Comparison of experimental and simulated reflectance data as a function of optical thickness of the organic layer and excitation wavelength for structure "A", which is optimized for the absorption in Alq<sub>3</sub>.

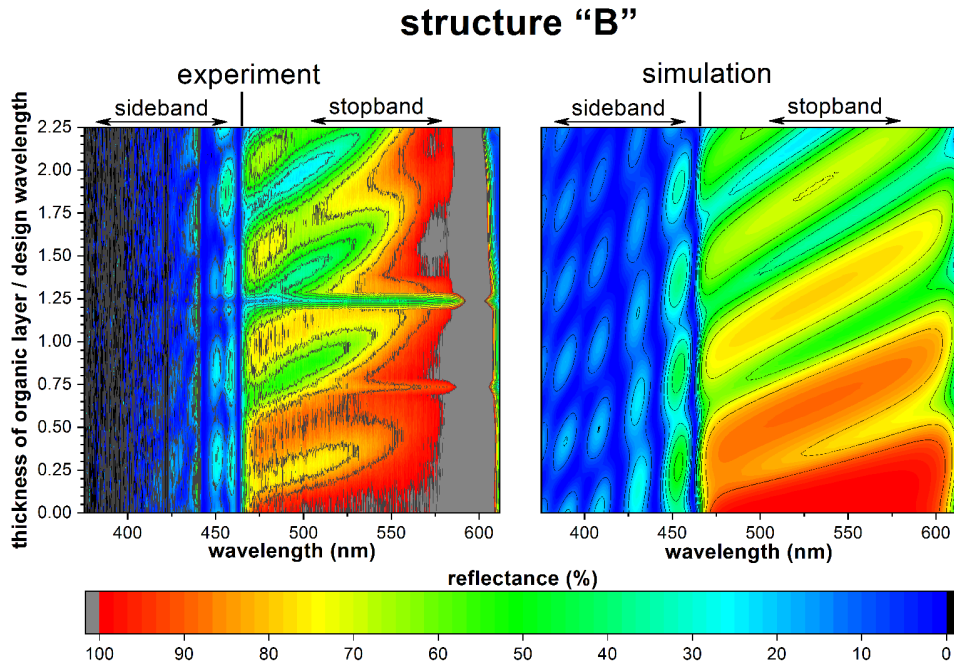


Figure 4. Comparison of experimental and simulated reflectance data as a function of optical thickness of the organic layer and excitation wavelength for structure "B", which is optimized for the absorption in DCM.

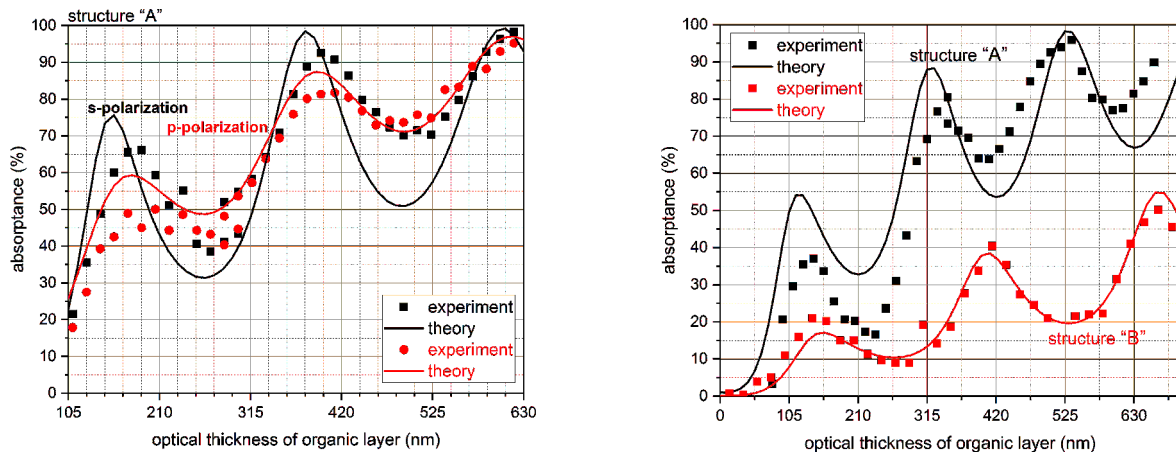


Figure 5. Left: Comparison of absorptance under oblique excitation as a function of optical thickness of the absorbing layer in structure “A” between s-polarized (black) and p-polarized (red) light. The experimental data is shown with squares/dots and the data from simulations with continuous lines. Right: Comparison of absorptance as a function of optical thickness of the organic absorbing layer between structure “A” and structure “B” for perpendicular excitation with the respective design wavelength of the structure. The experimental data is shown with squares and the data from simulations with continuous lines.

s-polarized light for an incident angle of  $45^\circ$  is shown in figure 5 on the left side, where it becomes obvious that they differ from each other significantly. As before the experimental and theoretical data are very similar.

Because of the oblique incidence of the beam, there are drastic changes in the optical properties of the underlying multilayer structure, but still the oscillations in absorptance for an increasing thickness of the absorbing layer are obvious. This indicates, that coherent absorption is still possible with s- and p-polarization, which show the same periodicity in these oscillations but with different amplitudes. For a layer thickness of around 610 nm the absorptance is close to 100% for s-polarized light and therefore really close to coherent perfect absorption.

### 3.3 Conclusion

For both structures “A” and “B” we could prove the presence of coherent absorption in  $\text{Alq}_3$  and DCM in the stopband of the respective sample. Because of the composition of the organic material the absorption was much stronger for  $\text{Alq}_3$  than for DCM. We could even achieve CPA in  $\text{Alq}_3$  as shown in figure 5 on the right side. Due to the small fraction of DCM in the absorbing material, it was not possible to show CPA in DCM within the thickness range of the produced structures, which does not mean that this would not happen for larger thicknesses. Furthermore, we note that the position of maxima and minima is not as closely related to the standing wave character of the light inside the organic layer due to the asymmetric structure design as well as nontrivial phase relations between the subsequent reflections from the DBR aside the design wavelength.<sup>22</sup> Finally we demonstrated that an oblique excitation still leads to coherent absorption, which is therefore not disturbed by the spatial separation of the reflected beams. Probably this comes from the spatially broad excitation with white light.

## 4. COHERENT PERFECT ABSORPTION FOR LASER EXCITATION

### 4.1 Non-linearities of CPA

Both previously investigated structure were also investigated under excitation with a laser to check if coherent absorption shows any non-linear effects. Numerous processes (e.g. ground state bleaching, excited state absorption, multi-photon excitation processes, etc.) could modify absorption in our structures and, since CPA strongly depends on absorption coefficient of the optically active organic layer, the CPA peak could show a substantial

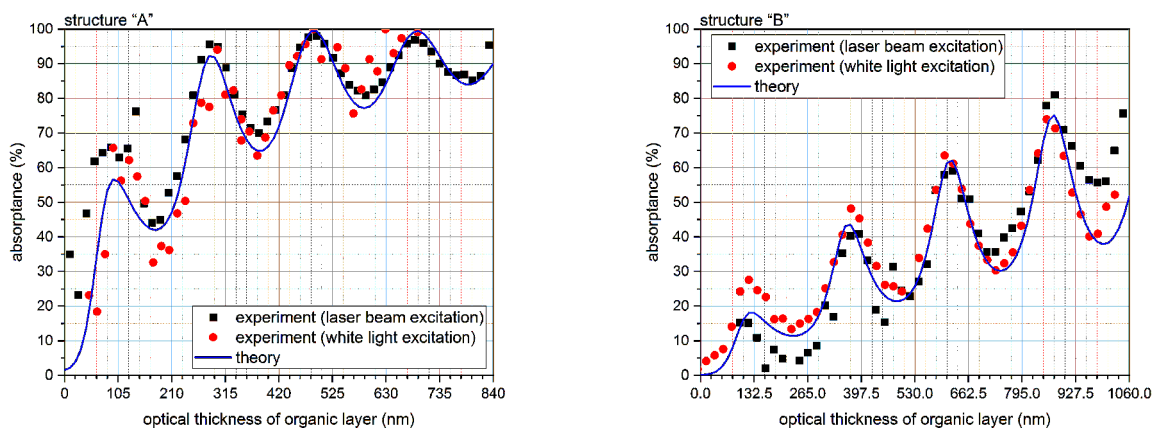


Figure 6. Comparison of absorbance as a function of optical thickness of the organic absorbing layer between perpendicular excitation with white and with a laser beam. The experimental data for structure “A” (left) and structure “B” (right) is shown with squares/dots and the data from simulations with continuous lines.

shift compared to previous experiments and the overall shape of the oscillations in absorbance could change a lot. From recent observations in our organic microcavity lasers we know that there might be some sort of saturation of population inversion in the same organic gain medium as it is used in structures “A” and “B”.<sup>23</sup>

#### 4.2 Comparison to white light excitation

Both structures are getting excited by a pulsed frequency doubled femtosecond laser beam from a regenerative amplifier system with an excitation wavelength of 404 nm. The resulting data from these measurements are shown in figure 6 for structure “A” and “B” each in comparison with simulated data from transfer-matrix calculations. From the similarities between experimental and theoretical data we can conclude the coherence length of 100 femtosecond pulses, generated by our amplifier system, exceeds the critical length that would be mandatory to get coherent absorption in our one-port device structure.

In comparison with the data from excitation with white light from a halogen lamp, shown in figure 6, there is no difference that would be worth mentioning, although we already know that there should be some saturation effect influencing the absorption. That this is not visible is probably due to fact, that we used the pumping beam not only for exciting but also for scanning the sample, meaning we are just observing effects in the absorption band of Alq<sub>3</sub> and DCM. In microcavity laser systems the lasing usually starts 40 picoseconds after the pumping starts, because the population inversion takes time to build first. In lasing experiments the saturation effects were seen in the lasing output. All in all we can conclude from these facts, that the saturation needs to take place in the emission band of either Alq<sub>3</sub> or DCM. Another possible explanation for the total absence of saturation in our experiments is the spot size of the excitation. The measured light in lasing experiments originates from the mode volume inside this cavities. This area is significantly smaller than the spot size of the pumping laser, which is used for the excitation. Analyzing the reflectance or absorbance of our one-port device structure uses the whole area of the laser spot and therefore the amount of saturated molecules inside the mode volume might simply be suppressed by the surrounding, non-saturated material. Because of the small fraction of DCM in the absorbing layer, this second explanation is a bit more unlikely than the first one, because the DCM should be saturated very easily.



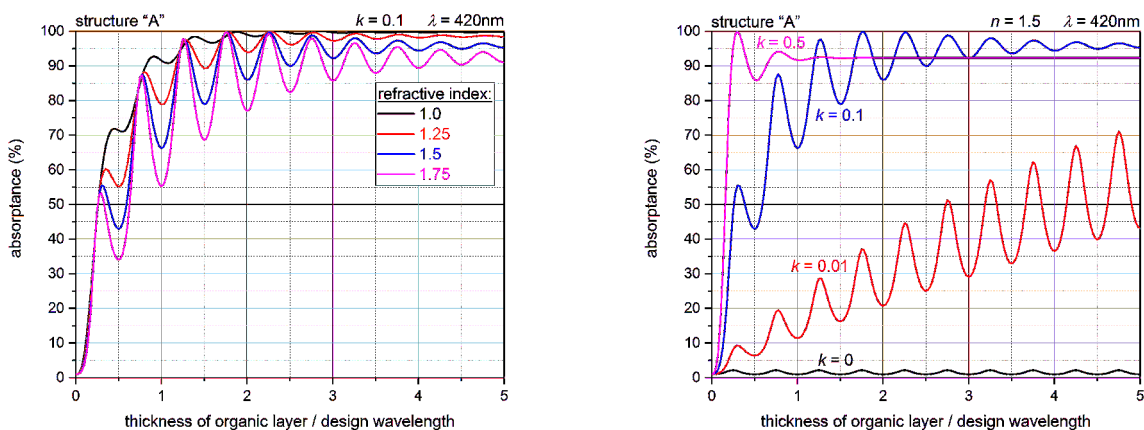


Figure 7. Absorbance in one-port device with wedged absorbing layer depending on the wedge thickness for different real (left) and imaginary (right) parts of the refractive index of the absorbing material.

## 5. DETERMINATION OF OPTICAL DISPERSION RELATIONS BY COHERENT ABSORPTION EFFECTS

### 5.1 Basic concept and implementation

So far, we used reflection as a function of wedged thickness to investigate coherent absorption, but it turned out, that this concept can be used to determine the optical dispersion relation. In order to do so, one needs a sample with a one-port device structure as shown in figure 1 (left). Essentially it needs a highly reflecting mirror on the bottom, for example a DBR, topped with a wedged layer of material, which should be investigated. One can also add an additional substructure on top of that, but this has to be kept as simple as possible and taken into account when evaluating the measurements.

The reflectivity in such a structure needs to be measured as a function of wedge thickness. For simplicity all further shown measurements are done with perpendicular illumination of the sample, carried out with a strongly focused white-light beam from a halogen lamp. It should be mentioned that it is also possible to perform the illumination under oblique incidence. The used wedge in our samples is approximately at  $6.7 \cdot 10^{-5}$  rad. This ensures that the wedge itself has no significant influence on reflection and transmission functions of the device under focusing conditions of our scanning beam.

Figure 7 shows the different influences of real and imaginary refractive index parts. An unequivocal allocation of a pair of  $n$ - and  $k$ -values to a given set of data depends on these unique impacts. Therefore it is possible to explicitly determine the complex refractive index of the absorbing material. Because the evaluation is done for every wavelength individually the dispersion relations can be determined even for a single wavelength only. This results from the fact that no model needs to be applied to the dispersion relations of the material. After measuring, the complex refractive index of the absorber can be extracted by combining the transfer matrix method and multivariate analysis in order to find the global minimum in deviation between measurement data and transfer matrix calculations. To perform these simulations the specific structure of the sample needs to be known. A common very basic problem in this kind of multivariate analysis is, that one can never be sure if a global or just a local minimum was reached.

### 5.2 Results and conclusion

The by this novel method obtained results for the complex refractive index are shown in comparison with results from ellipsometry measurements in figure 8 with the intention to evaluate their reliability.<sup>24,25</sup> The diagram shows the results for two samples with AlQ<sub>3</sub>:DCM as they were used already in previous sections. There were two samples with differently located stopbands used, because only in the stopband one can get reliable results

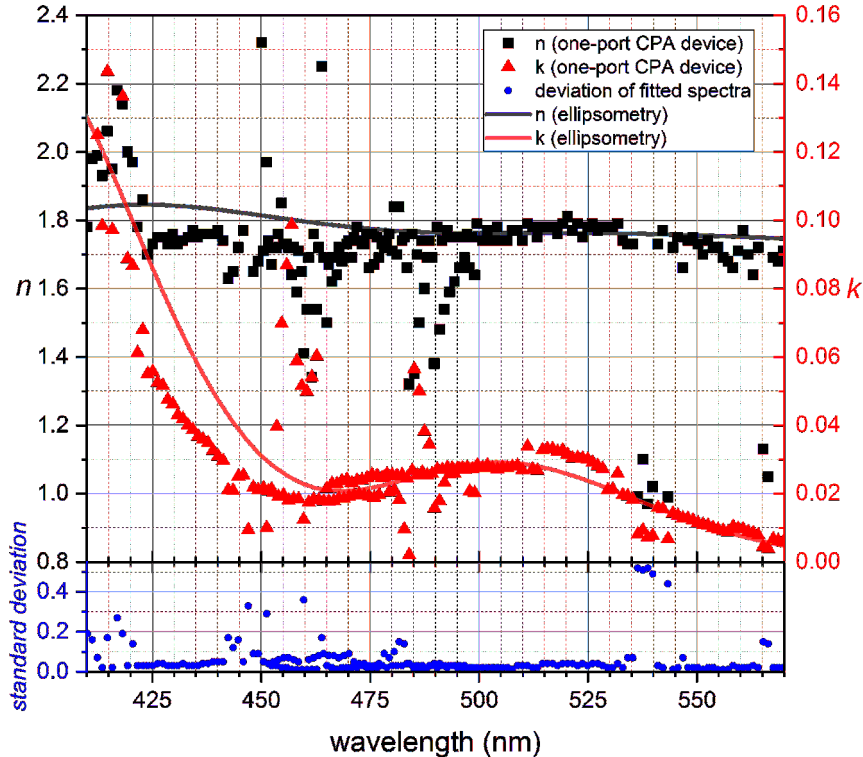


Figure 8. Comparison of optical dispersion relations by ellipsometry (lines) and novel method. Standard deviation of the fit of experimentally measured reflection data from transfer matrix approach is shown in the lower plot.

for the complex refractive index. Therefore the data of both samples is overlapping in the wavelength region between 450 nm and 475 nm and are in very good agreement with each other.

Based on the fact, that the investigated material consists primarily  $\text{Alq}_3$  with a small fraction of DCM, one would expect a major absorption peak around 400 nm from the  $\text{Alq}_3$  and a minor peak at 510 nm resulting from the DCM absorption. The imaginary part of the refractive index shown in figure 8, which is closely related to the absorption coefficient of the material, shows exactly this expected behaviour. Also the results from the novel methods are almost the same as the results from ellipsometry, which has already proven to deliver reliable results. Finally this leads to the conclusion, that our novel method can be used to accurately determine the dispersion relation of a material. Some values, especially at the end of the stopbands of the respective sample, are scattered a lot. This coincides with a large standard deviation and indicates, that the algorithm which was used for the evaluation simply failed to properly match experimental data with the transfer matrix calculations. One should also consider, that the  $n$ - and  $k$ -values from the novel method were all obtained for single wavelengths only without taking the neighbouring values into account. The evaluation algorithm could therefore still be improved a lot.

### ACKNOWLEDGMENTS

The authors are grateful to Christian Hänisch and Dr. Bolko Schöneich for carrying out ellipsometry measurements as well as to Christoph Schmidt for useful and stimulating discussions. The authors gratefully acknowledge funding and support of the DFG projects No. FR 1097/3-1, LE 747/53-1, and LE 747/55-1 and the Cluster of Excellence Center for Advancing Electronics Dresden.

## REFERENCES

- [1] Brédas, J., Sargent, E. H., and Scholes, G. D., “Photovoltaic concepts inspired by coherence effects in photosynthetic systems,” *Nature materials* **16**, 35–44 (2017).
- [2] Tischler, J. R., Bradley, M. S., and Bulovic, V., “Critically coupled resonators in vertical geometry using a planar mirror and a 5nm thick absorbing film,” *Optics Letters* **31**, 2045–2047 (July 2006).
- [3] Teperik, T. V., García De Abajo, F. J., Borisov, A., Abdelsalam, M., Bartlett, P. N., Sugawara, Y., and Baumberg, J. J., “Omnidirectional absorption in nanostructured metal surfaces,” *Nature photonics* **2**, 299 (2008).
- [4] Auguié, B., Bruchhausen, A., and Fainstein, A., “Critical coupling to tamm plasmons,” *J. Opt.* **17**(3), 035003 (2015).
- [5] Deb, S., Dutta Gupta, S., and Banerji, J., “Critical coupling at oblique incidence,” *Journal of Optics A: Pure and Applied Optics* **9**, 555–559 (2007).
- [6] Dutta Gupta, S., Deshmukh, R., Gopal, A. V., Martin, O. J. F., and Dutta Gupta, S., “Coherent perfect absorption mediated anomalous reflection and refraction,” *Optics letters* **37**, 4452–4454 (2012).
- [7] Ding, B., Qiu, M., and Blaikie, R. J., “Manipulating light absorption in dye-doped dielectric films on reflecting surfaces,” *Opt. Express* **22**(21), 25965–25975 (2014).
- [8] Häggglund, C., Apell, S. P., and Kasemo, B., “Maximized optical absorption in ultrathin films and its application to plasmon-based two-dimensional photovoltaics,” *Nano letters* **10**, 3135–3141 (2010).
- [9] Pu, M., Feng, Q., Wang, M., Hu, C., Huang, C., Ma, X., Zhao, Z., Wang, C., and Luo, X., “Ultrathin broadband nearly perfect absorber with symmetrical coherent illumination,” *Optics Express* **20**, 2246–2254 (2012).
- [10] Li, S., Luo, J., Anwar, S., Li, S., Lu, W., Hang, Z. H., Lai, Y., Hou, B., Shen, M., and Wang, C., “Broadband perfect absorption of ultrathin conductive films with coherent illumination: Superabsorption of microwave radiation,” *Physical Review B* **91**(220301) (2015).
- [11] Chong, Y. D., Ge, L., Cao, H., and Stone, A. D., “Coherent perfect absorbers: Time-reversed lasers,” *Physical Review Letters* **105**(053901) (2010).
- [12] Wan, W., Chong, Y., Ge, L., Noh, H., Stone, A. D., and Cao, H., “Time-reversed lasing and interferometric control of absorption,” *Science* **331**, 889–892 (2011).
- [13] Longhi, S., “Backward lasing yields a perfect absorber,” *Physics* **3**, 61 (2010).
- [14] Longhi, S., “Pt-symmetric laser absorber,” *Physical Review A* **82**, 031801 (September 2010).
- [15] Born, M. and Wolf, E., [*Principles of optics*], Pergamon Press, 7th edition ed. (1999).
- [16] Dey, S., “Coherent perfect absorption using gaussian beams,” *Optics Communications* **356**, 515–521 (2015).
- [17] Kozlov, V. G., Bulović, V., Burrows, P. E., and Forrest, S. R., “Laser action in organic semiconductor waveguide and double-heterostructure devices,” *Nature* **389**, 362–364 (1997).
- [18] Koschorreck, M., Gehlhaar, R., Lyssenko, V. G., Swoboda, M., Hoffmann, M., and Leo, K., “Dynamics of a high-Q vertical-cavity organic laser,” *Appl. Phys. Lett.* **87**, 181108–1–3 (2005).
- [19] Schütte, B., Gothe, H., Hintschich, S. I., Sudzius, M., Fröb, H., Lyssenko, V. G., and Leo, K., “Continuously tunable laser emission from a wedge-shaped organic microcavity,” *Appl. Phys. Lett.* **92**, 163309 (2008).
- [20] Yariv, A. and Yeh, P., [*Photonics: optical electronics in modern communications*], Oxford University Press (2006).
- [21] Baldacci, L., Zanotto, S., and Tredicucci, A., “Coherent perfect absorption in photonic structures,” *A. Rend. Fis. Acc. Lincei* **26**, 219–230 (2015).
- [22] Yu, N. and Capasso, F., “Flat optics with designer metasurfaces,” *Nature Materials* **13**, 139–150 (January 2014).
- [23] Brückner, R., Sudzius, M., Fröb, H., Lyssenko, V. G., and Leo, K., “Saturation of laser emission in a small mode volume organic microcavity,” *Journal of Applied Physics* **109**(103116) (2011).
- [24] Tompkins, H. G., [*A User’s Guide to Ellipsometry*], Academic Press Inc., 1250 Sixth Avenue, San Diego, CA 92101 (1993).
- [25] Fujiwara, H., [*Spectroscopic Ellipsometry: Principles and Applications*], Wiley (2007).